ACS OMEGA

http://pubs.acs.org/journal/acsodf

Article

Experimental Investigation on the Penetrability Mechanism of Gel Slug During Well Completion Processes

Xiangji Dou, Yong Du, Yisong Zhang, and Kun Qian*

Cite This: *ACS Omega* 2023, 8, 23112−23119

Read Online

ACCESS | Metrics & More | Article Recommendations

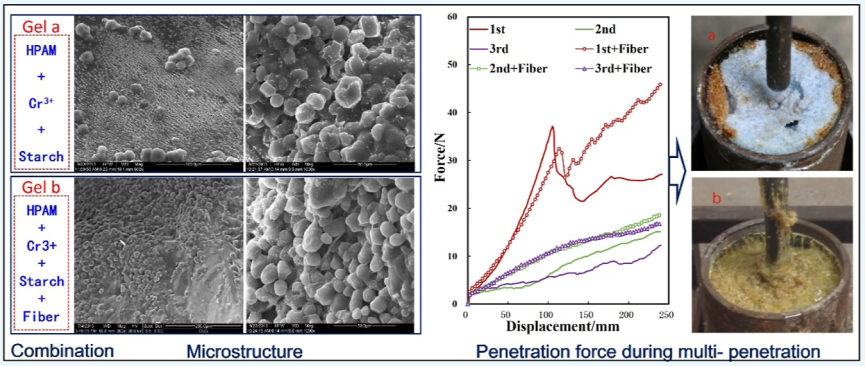

ABSTRACT: Reservoir formation damage is an essential problem which troubled oil and gas well production, a smart packer is a promising technology to maintain sustainable development for the oil and gas fields. Currently, the "gel valve" technology has been proved to be feasible with gel slug to seal casing and descend the completion pipe string, while the systemic performance of ideal gel is still not clear. In the underbalanced completion stage with the gel valve, the downward completion string needs to penetrate the gel slug to form an oil and gas passage in the wellbore. The penetration of rod string to gel is a dynamic process. The gel-casing structure often shows a time-dependent mechanical response, which is different from the static response. In the process of penetration, the interaction force between the rod and gel is not only related to the properties of the interface between gel and string but also affected by the moving speed, rod diameter, and thickness of the gel. The dynamic penetration experiment was carried out to determine the penetrating force varied with depth. The research showed that the force curve was mainly composed of three parts, the rising curve of elastic deformation, decline curve for the surface worn out, and another curve of the rod wear into. By changing the rod diameter, gel thickness, and penetration speed, the change rules of forces in each stage were further analyzed, which would provide a scientific basis for a well completion design with a gel valve.

1. INTRODUCTION

The global demand for oil and natural gas resources is increasing daily, which brings a great challenge to the oil and natural gas companies due to the increasing difficulties of well drilling and completion,[1−3] especially for the exploration and development of low permeability of oil and gas fields. The development of low permeability reservoirs has become a major trend presently.[4−6] With the continuous improvement of exploration technology, the quality of the newly developed oil and gas reservoirs will become worse and worse, and the proportion of low permeability reserves will become higher and higher.[7−9] In low permeability reservoirs, the formation is very vulnerable to pollution and damage, and the production of oil and gas wells is low due to the tight cementation, muddy and fine minerals, low porosity, stress sensitivity, and low effective permeability.[10−14] Therefore, it is very important to protect reservoirs, reduce and avoid pollution for long-term development, and stable production of low permeability oil and gas fields.[15−17]

Generally, it is necessary to use killing fluid or blow out pressure to ensure the safety of downhole operation before drilling and completion.[18−20] However, it is inevitable to invade reservoirs in killing operation, resulting in a sharp decline in permeability and oil and gas production due to the change of physical and chemical properties of oil and gas reservoirs and plugging of pores by solid particles.[21,22] According to the data statistics, each well killing operation can reduce production by 20%.[23,24] Meanwhile, the pressure blow-out will lead to the pressure drop of local formation, damaging the formation

Received: April 12, 2023
Accepted: June 6, 2023
Published: June 15, 2023

structure and well pattern pressure distribution , and reduce the formation productivity. Therefore, killing and blowout operations are not conducive to the sustainable development of oil and gas resources but also not beneficial for the development of low permeability and low production of sensitive reservoirs. In order to protect low permeability reservoirs, non-killing technology has been widely used in underbalanced drilling and completion, perforation, oil testing, testing, and workover operations in oil and gas fields. At present, the popularization and application rate of non-killing technology in major oil and gas producing areas in North America and the Middle East has reached more than 90%, bringing enormous economic and social benefits. However, the high cost of well-killing operation and the problems in the actual operation process, such as the switch not working and sealing not being strict, seriously restricts the large-scale application of non-well-killing technology. In order to solve the above problems, the concept of "gel valve", which using a section of gel to seal the wellbore and form a dynamic seal with the string, was proposed by the Tuha Oilfield.[25−27] In the concept, the chemical intelligent gel was used instead of casing plugger and other complex devices, which has significance in reducing operation cost, simplifying the process, and protecting the reservoir. The gel is a kind of soft material, whose properties are between liquid and solid. It is most likely to realize the function of the valve.[28−30] On the one hand, the gel has a certain strength and adhesive property, which is easy to produce large deformation under the external forces and adhere to the casing wall to block fluid; on the other hand, the strength of gel is much weaker than the general solid, which is conducive not only to descend the rod string or downhole tools but also to achieve dynamic sealing.[31,32] It can be concluded that the realization of the function of the "gel valve" is closely related to the mechanical properties of soft materials, such as gel.

Soft matter mechanics is the frontier of solid mechanics. The special properties, research methods, and mechanics theory of soft matter has always been the focus of international research.[33−36] However, due to the particularity and diversity of the microstructure, morphology, and mechanical properties of soft materials, there is no complete set of soft material performance testing and evaluation methods, and the related theories are also imperfect. In view of the above problems, the laboratory experiments were utilized to obtain the compressive strength and penetration force of gel valve, which takes the non-killing process into account. Then, the sealing and penetration characteristics of the gel was analyzed. In addition, by comparing the microstructure and macro-mechanical parameters of different colloids, the influence of structure on the properties of the gel was discussed, which provided a reference for the modification and development of the gel.

2. EXPERIMENTAL DESCRIPTION

2.1. Experimental Equipment. In the experiments, the inner diameter and outer diameter of the cast were 84.5 and 95.0 mm, respectively. The thickness of the gel slug was 50∼300 mm. There were four different sizes of the flat rod in the experiment, namely, 13.5, 20, 25, and 30 mm, the maximum penetration speed of the flat rod was 1000 mm/min (Figure 1).

2.2. Sample Preparation. The gel formed by the cross-linking reaction of polyacrylamide (HPAM) with high valence metal-ion Cr^{3+} was a soft solid, which was insoluble in water. Its network structure determined the high strength and fluidity of the gel. In the experiment, the components of the gel included

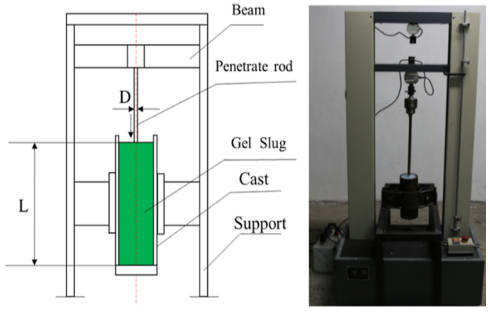

Figure 1. Penetration experimental equipment (Photograph courtesy of Yong Du. Copyright 2023.).

10% HPAM, 10% starch, 1% Cr^{3+} cross-linking agent, and 5% fiber. Five different solutions were made by different combinations: (1) HPAM; (2) HPAM + Cr^{3+} cross-linking agent; (3) HPAM + Cr^{3+} cross-linking agent + fiber; (4) HPAM + Cr^{3+} cross-linking agent + starch; and (5) HPAM + Cr^{3+} cross-linking agent + starch + fiber. Then, the solution was placed in a 101-1 type electric blast drying oven (Beijing Kewei Yongxing Instrument Co., Ltd.) for heating and gelled at 60 °C for 12 h. The microstructure of the gel was scanned by scanning electron microscopy (SEM), and the microstructures are shown as Figure 2.

According to the SEM results, the HPAM morphology of sample 1 was flat and uniform. After cross-linking reaction between HPAM and Cr^{3+} ions, a network structure was formed in sample 2, each part was cross-linked and extremely uneven. After the fiber was added, the structure of sample 3 became regular and uniform, and it was "honeycomb" (as shown in Figure 2c). When starch was used in place of the fiber, the starch granules filled in the gel were bonded to each other, and the morphology of sample 4 is expressed as a "sea-island" structure (as shown in Figure 2d). After the starch and fiber were added successively, starch granules in sample 5 were dispersed and arranged in a regular manner, which was the result of the cellulose providing a large steric hindrance and hydrogen bonding with the starch (as shown in Figure 2e).

Through the above comparative analysis, it can be seen that the cross-linking reaction between HPAM and Cr^{3+} ions produced a disordered network structure, the starch granules filled inside mainly serve as a skeleton support, and the structure can be made regular by adding fibers. In the following discussion, sample 4 and sample 5 were used to have deep research on the penetrability mechanism of gel slug.

In order to understand the dynamic viscoelastic properties of these gel slug, the small amplitude oscillatory shear stress scanning of the gel was performed by a RheoStree 600 (Haake, Germany) stress-controlled rheometer. The relationship between energy storage modulus G' and loss modulus G'' and fluctuating frequency ω of sample 4 and sample 5 are indicated in Figures 3−4. In experiments, the energy storage modulus refers to the ability of the gel system to store energy in a period under alternating stress, usually representing the elasticity of the gel. The greater the value is, the greater the elasticity of the gel is. The loss modulus refers to the ability of a colloidal system to dissipate energy in a changing period, usually representing the viscosity of the gel. The larger the value is, the better the viscous fluidity of gel is. When the gel system is in a liquid-like state, its storage modulus is much smaller than the loss modulus; when the gel system is in the solid-like state, its storage modulus is much larger than the loss modulus.

https://doi.org/10.1021/acsomega.3c02494
ACS Omega 2023, 8, 23112−23119

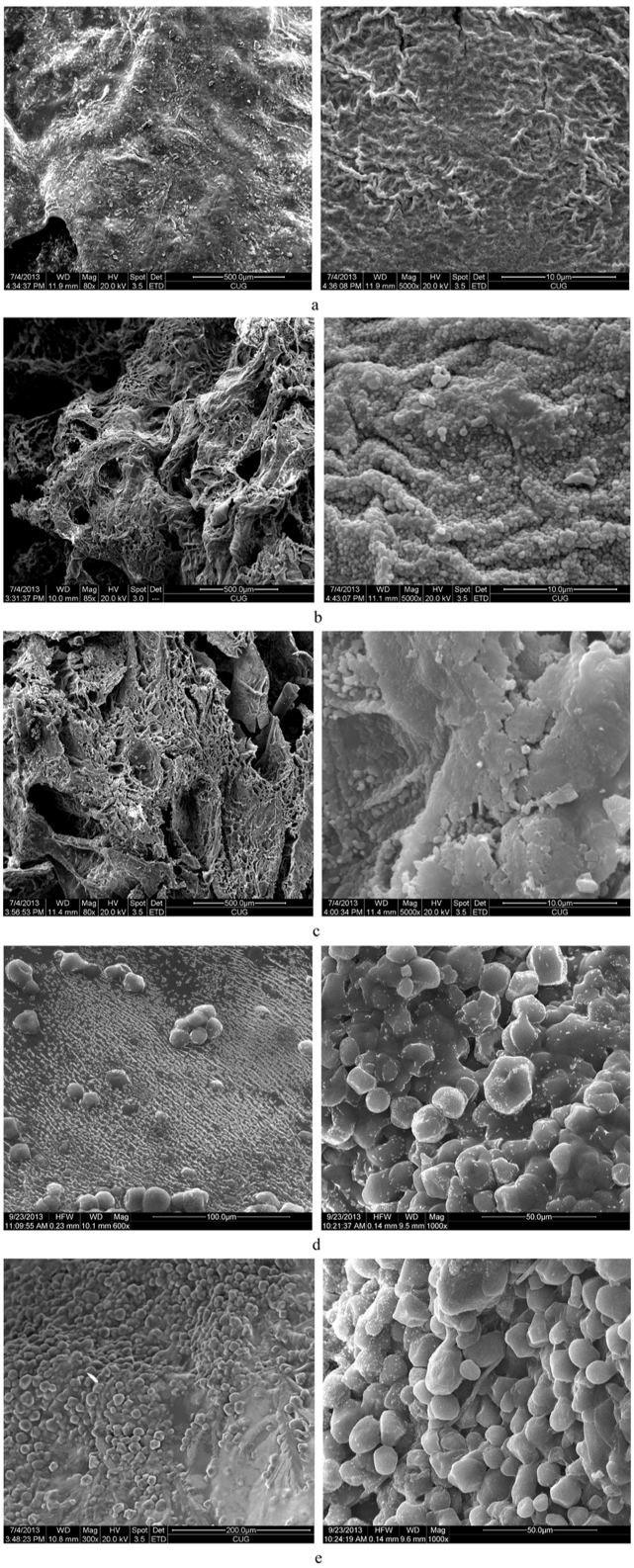

Figure 2. Microstructure of different gels. (a) Sample 1 (HPAM). (b) Sample 2 (HPAM + Cr^{3+}). (c) Sample 3 (HPAM + Cr^{3+} + fiber). (d) Sample 4 (HPAM + Cr^{3+} + starch). (e) Sample 5 (HPAM + Cr^{3+} + starch + fiber).

As demonstrated in Figure 3, the storage modulus was greater than the loss modulus in most cases when the oscillation frequency ranged from 0.01 to 100 rad/s, and the gel system showed obvious solidification. The storage modulus and loss

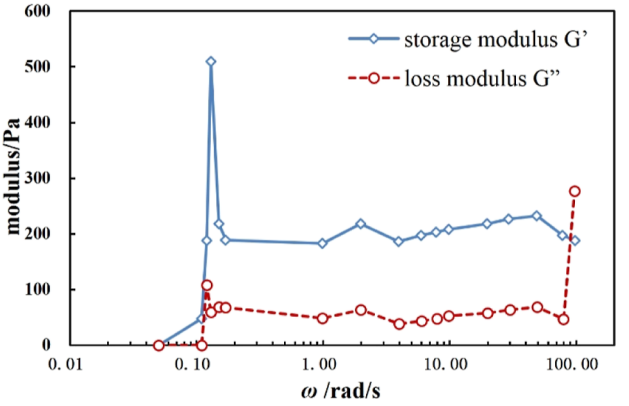

Figure 3. Change of storage modulus G' and loss modulus G'' with a frequency of sample 4.

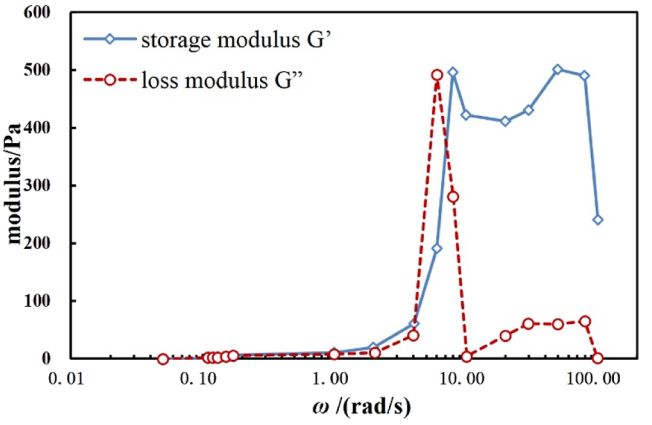

Figure 4. Change of storage modulus G' and loss modulus G'' with a frequency of sample 5.

modulus increased sharply in the low-frequency region and then decreased sharply. With the further increase of the oscillation frequency, the storage modulus increased slowly and the loss modulus basically remained unchanged. The reason was that the vibration of the polymer chain resonated with the vibration of the external frequency with the increase of the oscillation frequency, which made the viscoelasticity of the gel system increase to the maximum. Then with the further increase of the oscillation frequency, the vibration destroyed the network structure formed by the polymer chain, and the viscoelasticity was weakened. As indicated in Figure 4, when the fiber was added in the gel, with the increase of resonance frequency, the storage modulus was maintained at a higher level in a wider frequency range. The loss modulus that approached the maximum value of the storage modulus at the resonance frequency was 4 rad/s and also increased significantly when the resonance frequency was over 10 rad/s, which meant that the elasticity and viscosity of the gel system were enhanced because the cellulose surface was rich in hydroxyl groups, and there was a strong hydrogen bond between the cellulose surface and polyacrylamide and starch.

2.3. Experimental Schedule. In the experiments, the gel slug was formed in the cast fixed on the support, and the screw was driven by the servo motor to move the beam and the rod downward together (as shown in Figure 1). The force acting on the rod with constant velocity through a certain thickness of gel was measured. The penetration rate, rod diameter, and gel thickness were changed to determine the penetrability of the gel

https://doi.org/10.1021/acsomega.3c02494
ACS Omega 2023, 8, 23112−23119

Table 1. Materials and Condition of the Penetrability Tests

test no	materials	penetration rate/(mm/min)	rod diameter/mm	gel thickness/mm	penetration times
1	sample 4	1000	13.5	50/100/150/200/250/300	1
2	sample 4	250/500/750/1000	13.5	100	1
3	sample 4	1000	13.5/20/25/30	100	1
4	sample 4/5	1000	13.5	100/200/300	1
5	sample 4/5	1000	13.5	300	3

slug under different conditions and the maximum force required. The experimental materials and conditions are presented in Table 1.

3. RESULTS AND DISCUSSION

3.1. Penetrability Mechanism of Gel Slug. The process of the rod penetrating the gel is shown in Figure 5. In the

Figure 5. Process of rod penetrating gel slug of sample 4 (Photograph courtesy of Yong Du. Copyright 2023.). (a) Gel was concavely deformed but not broken at the beginning of the penetration. (b) Central area of the gel surface was recessed as the rod moved down. (c) Surrounding colloid moved to the center area. (d) Penetration tunnel shrank after the lifting of the rod.

experiment, the diameter of the rod was 13.5 mm, the penetrate velocity was 1000 mm/min, and the thickness of the gel slug was 300 mm. When the rod penetrated the gel at a constant speed, the gel was concavely deformed but not broken, and the upper surface was in a stretched state (as shown in Figure 5a). As the rod moved down, the central area of the gel surface was recessed, and the surrounding colloid moved to the center area, which caused the tearing action on the surrounding cementation interface and degumming (as shown in Figure 5b,c). When the rod broke the surface of the gel, cracks were generated inside the colloid and the cracks extended as the rod moving down. It can be seen from Figure 5d that after the lifting of the rod, the elastic recovery occurred inside the colloid, and the penetration tunnel shrank.

Figure 6 is the force−displacement curve of the penetrating process. As indicated in the curve, the force increased quadratically with the downward displacement in the elastic deformation stage when the gel surface was pressed by the rod. When the rod broke through the gel surface, the force decreased sharply, then the rod was in a stable penetration process. At this stage, the colloid rebounded upward and the adhesive friction

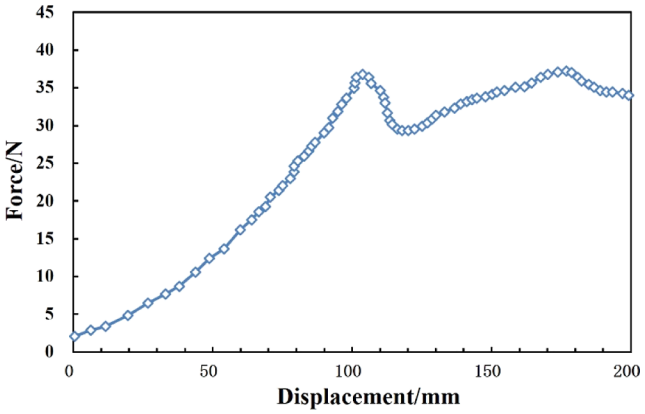

Figure 6. Penetration force−displacement curve of penetration process (sample 4).

increased with the depth of the rod. Therefore, the force of the rod increased continuously. Then, the stiffness decreased due to the weakening of the colloid rebound and the shortening of the thickness of the unbroken gel, the rising speed of the force slowed down and the curve was relatively flat.

From the analysis above, it can be concluded that the penetration force curve of the gel slug was mainly composed of the rising section of the elastic deformation of the gel, the sharp falling section after the surface was broken, and the stable penetration section of the rod. Meanwhile, the maximum load before breaking the surface of the gel, the minimum load after breaking the lower surface of the gel, and the change rate of stable penetration load were key factors to determine the dynamic mechanical behavior of rod penetrating slug. It was necessary to further study the effects of the thickness of gel, penetration velocity, and rod diameter on the penetration law of gel slug.

3.2. Analysis of Influence Factors. *3.2.1. Effect of the Thickness of the Gel Slug.* In this group of experiments, different thicknesses of gel slugs were made to investigate the effect of the thickness of gel slug on the penetration force. The diameter of the rod was 13.5 mm and the penetrate velocity was 1000 mm/min. The thickness of gel slug were 50, 100, 150, 200, 250, and 300 mm. Figure 7 is the force−displacement curve of the penetrating process under different thicknesses of gel slug. As demonstrated in Figure 7, when the thickness of the gel exceeded 100 mm, the change of penetration force had the same tendency, and the force mainly experienced three stages of "up−down−up". When the rod broke through the lower surface of the gel slug, the resistance of the rod decreased sharply again. The rod was subjected to more stable adhesive resistance and dynamic friction during the subsequent movement, so the force tended to be gentle.

Figure 8 is the force and downward displacement of the surface pierced by different thicknesses of slugs. When the slug thickness was 50 mm, the force needed to break through the surface was 23.7 N. When the slug thickness exceeded 100 mm,

https://doi.org/10.1021/acsomega.3c02494
ACS Omega 2023, 8, 23112−23119

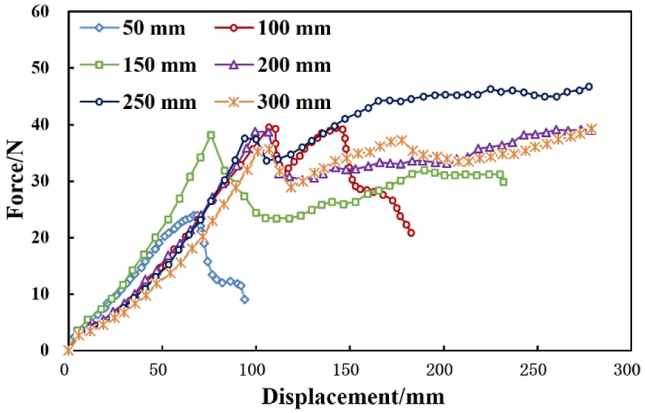

Figure 7. Penetration force−displacement of penetration processes with different gel thickness.

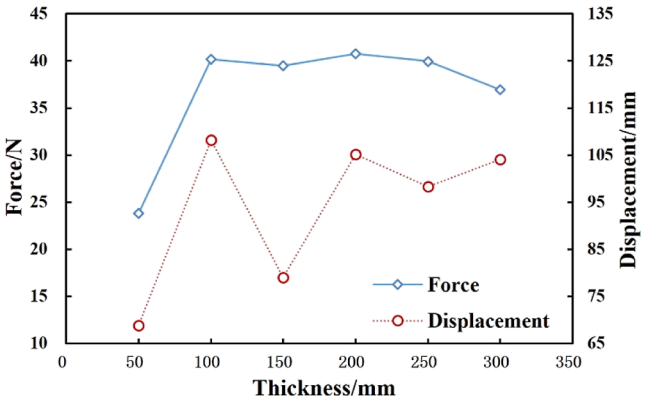

Figure 8. Surface broken force of penetration processes with different gel thicknesses.

the force fluctuated within a range of 36.8 N and increased gradually. In addition, the force curve in 50 and 150 mm of thickness shifted to the left (Figure 7), which indicated that the colloidal surface cracked under a smaller rod displacement. The cementation between the colloid and the inner wall varied in different tests. When the cementation between the colloid and the inner wall of the casing was stronger, the restraint effect of the surrounding wall on the concave deformation of the gel surface was greater, and the surface preferred to be broken with less displacement of the rod.

3.2.2. Effect of the Penetration Speed. When the rod diameter was 13.5 mm, and the thickness of gel slug was 100 mm, the penetration force−displacement curve under different penetration speeds is demonstrated in Figure 9. As indicated in Figure 10, the higher the rod penetration speed was, the greater the force was needed for the rod to penetrate the gel surface, and the force in the stable penetration process was also significantly increased. There was a linear relationship between the force acting on the surface and the velocity of the rod.

3.2.3. Effect of Rod Diameter. When the penetration speed was 1000 mm/min, and the thickness of gel slug was 100 mm, the penetration force−displacement curve under different rod diameters is demonstrated in Figure 11. It can be seen that the force required to break through the gel surface increased with the increase of the rod diameter. When the rod diameter was less than 20 mm, the force changed little, but the force increased linearly when the rod diameter exceeded 20 mm (Figure 12).

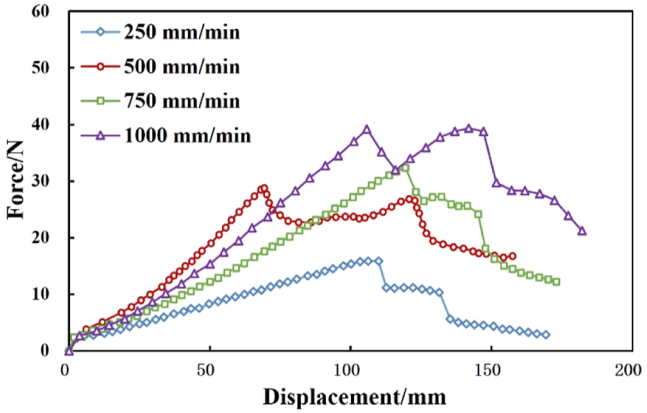

Figure 9. Penetration force−displacement curves of penetration processes with different speeds.

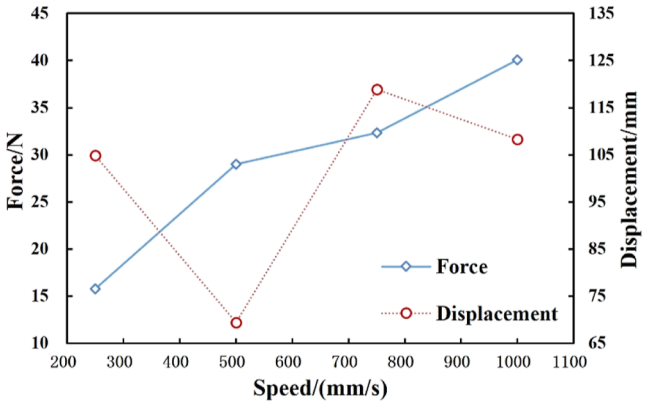

Figure 10. Surface broken force of penetration processes with different speeds.

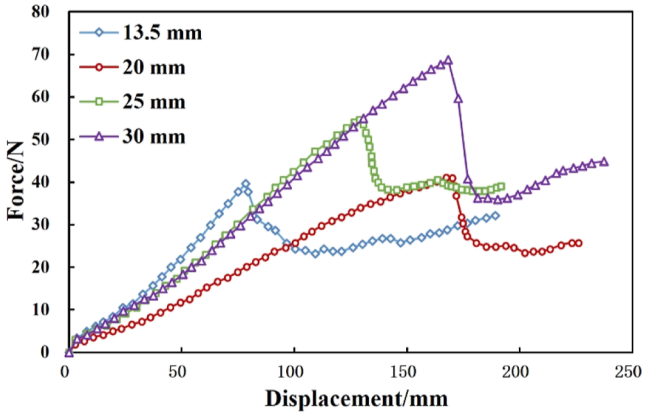

Figure 11. Penetration force−displacement curves of penetration processes with rods of different diameters.

3.2.4. Effect of the Addition of Fiber. As stated in Section 2.2, the fiber had a great effect on the mechanical property of gel slug. In these groups of experiments, the influence of fiber on the penetrability of gel slug was analyzed with sample 5. Under the certain conditions that the rod diameter was 13.5 mm and the penetration speed was 1000 mm/min, the penetration force of the slug before and after adding fiber is shown as Figure 13. It can be concluded that the gel toughness was enhanced after adding fibers, and the deformation of the surface was larger before it was broken, which made the force curve shift to the

https://doi.org/10.1021/acsomega.3c02494
ACS Omega 2023, 8, 23112−23119

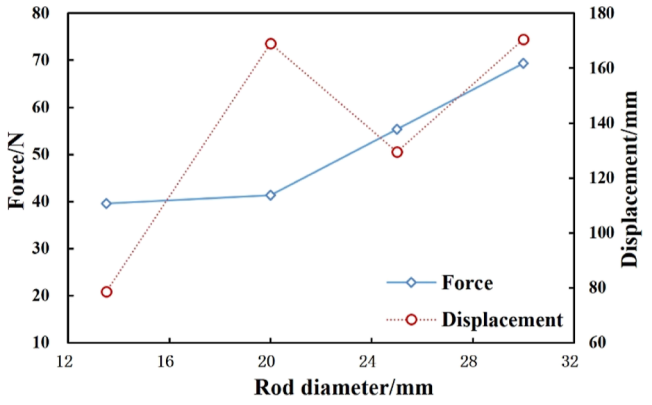

Figure 12. Surface broken force of penetration processes with rods of different diameters.

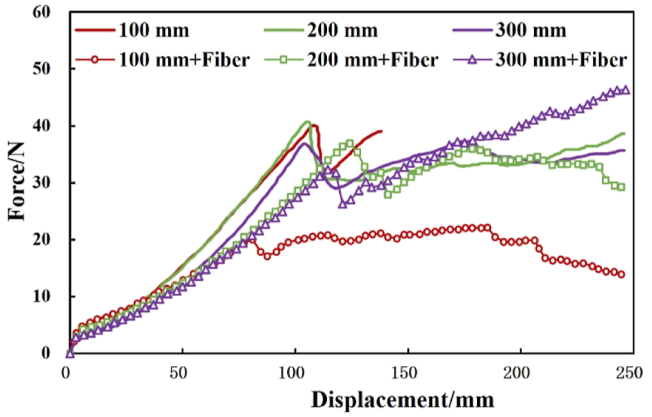

Figure 13. Penetration forces−displacement curves of penetration processes with no-fiber gel and fiber gel.

right. On the other hand, the breaking force of the rod decreased after adding fibers, and the penetration is relevant to the cementation condition between the gel and fiber. The fiber has good ductility and toughness, which can increase the toughness of the gel. However, when the fiber was stretched to a certain length, the fibers would lose ductility and break. Thus, the increase in toughness of the gel with fibers would occur within a certain range of gel deformation. Once the gel deformation exceeds to the range, the fiber would lose efficacy. When the thickness of the gel slug with the fiber was 100 mm, the cementation condition is much weaker due to the thin gel thickness. So, the gel broke with less displacement and the breaking force of the rod reduced obviously.

During drilling and completion, the drill pipe will pass through the gel slugs many times. Therefore, the mechanical properties of gel slugs after repeated penetration were studied. During the experiment, the mechanical properties of the gel slug after three penetrations were analyzed. After three penetrations, the gel slug still had good elastic recovery, so that the perforation channel was basically in a "closed state" (Figure 14). Influenced by the downward impact effect and the upward adhesive shear effect of the rod, some pits and cracks appeared in the surface of the gel (Figure 14a). After adding the fibers, the viscosity and toughness of the gel were enhanced, showing a "paste" state, and small groups of colloids were attached to the surface of the rod (as shown in Figure 14b). It can be seen that the contact and interaction between the colloid and the moving rod string were enhanced after adding the fiber, and the rod string showed a

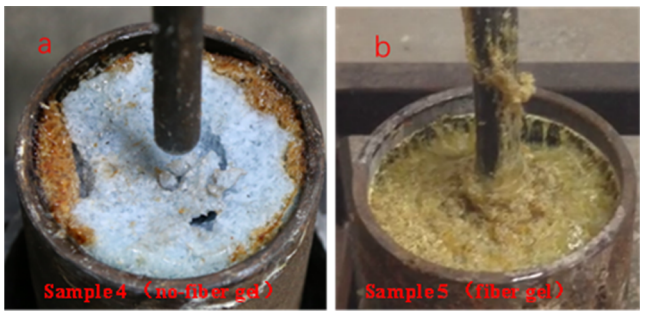

Figure 14. Slug surfaces after multi-penetration processes with no-fiber gel (a) and fiber gel (b) (Photograph courtesy of Yong Du. Copyright 2023.).

certain degree of "self-healing" after being lifted, which was expected to realize the dynamic seal between the slug and the downhole rod string or the downhole tool.

Figure 15 indicates the force−displacement relationship of multi-penetration and multi-lift. It could be found that in the

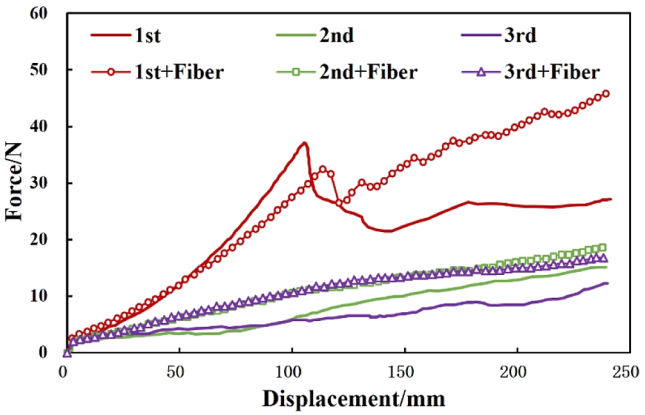

Figure 15. Force−displacement curves of multi-penetration processes.

second and third penetrations, the force mainly came from the frictional resistance during the penetration process, which was approximately linear with the displacement. With the increase of penetration times, the third penetration resistance was obviously smaller than the second one due to the colloid shedding and elasticity weakening around the hole. However, for the fiber toughened slug, the force curves of the two penetrations coincided basically, which indicated that the slug had better structural stability in the latter two penetrations.

4. CONCLUSIONS

In view of the application requirement of gel slug in non-killing operation and underbalanced drilling and completion, the sealing characteristics and penetrability of gel system were studied, which laid the foundation for the development of gel slug technology. The conclusions were as follows.

(1) Through the dynamic tests of rod penetrating gel, the change of rod action force during the penetration process was measured. Before the upper surface of the gel was broken, the action force increased linearly with the increase of deformation; when the gel was broken, the action force decreased sharply and the interface effect was larger; during the rod−column stable penetration process, the resistance increased continuously.

https://doi.org/10.1021/acsomega.3c02494
ACS Omega 2023, 8, 23112−23119

(2) The toughness of gel increased after adding fibers, and the deformation of the slug was larger before the surface was broken by the rod. The increase in toughness of the gel with fibers would occur within a certain range of gel deformation. Once the gel deformation exceeds the range, the fiber would lose efficacy. When the thickness of the gel slug with the fiber was 100 mm, the cementation condition is much weaker due to the thin gel thickness. Moreover, the slug had greater structural stability during multiple penetration, and it was expected to achieve dynamic seal in the process of rod string entry.

AUTHOR INFORMATION

Corresponding Author

Kun Qian − *School of Petroleum and Natural Gas Engineering, Changzhou University, Changzhou 213164, China;* orcid.org/0000-0002-6803-7120; Email: qiankun@cczu.edu.cn

Authors

Xiangji Dou − *School of Petroleum and Natural Gas Engineering, Changzhou University, Changzhou 213164, China*

Yong Du − *School of Petroleum and Natural Gas Engineering, Changzhou University, Changzhou 213164, China*

Yisong Zhang − *School of Petroleum and Natural Gas Engineering, Changzhou University, Changzhou 213164, China*

Complete contact information is available at: https://pubs.acs.org/10.1021/acsomega.3c02494

Notes

The authors declare no competing financial interest.

ACKNOWLEDGMENTS

This research is supported by the National Natural Science Foundation of China, Funding Name: Study on the Microscopic Phase Behavior and Migration Mechanism of CO_2 and Multicomponent Alkanes in Shale Dynamical Nanopore (no. 52004038).

REFERENCES

(1) Antonio, L.; Barrios, O. D.; Martinez Rodriguez, G. A. Swelling Packer Technology Eliminates Problems in Difficult Zonal Isolation in Tight-Gas Reservoir Completion. In *Latin American & Caribbean Petroleum Engineering Conference*; Society of Petroleum Engineers: Buenos Aires, Argentina, 2007; p 4.

(2) Bachu, S.; Gunter, W. D.; Perkins, E. H. Aquifer disposal of CO_2: Hydrodynamic and mineral trapping. *Energy Convers. Manage.* **1994**, *35*, 269−279.

(3) Carson, J. P.; Kuprat, A. P.; Jiao, X.; Dyedov, V.; del Pin, F.; Guccione, J. M.; Ratcliffe, M. B.; Einstein, D. R. Adaptive generation of multimaterial grids from imaging data for biomedical Lagrangian fluid−structure simulations. *Biomech. Model. Mechanobiol.* **2010**, *9*, 187−201.

(4) Offenbacher, M.; et al. Swellable Packer Fluids Designed for Zonal Isolation in Openhole Completions. In *SPE European Formation Damage Conference and Exhibition*; Society of Petroleum Engineers: Budapest, Hungary, 2015; p 10.

(5) María-Cervantes, A.; Conesa, H. M.; González-Alcaraz, M. N.; Álvarez-Rogel, J. Erratum to "Rhizosphere and flooding regime as key factors for the mobilisation of arsenic and potentially harmful metals in basic, mining-polluted salt marsh soils" [Appl. Geochem. 25 (2010) 1722−1733]. *Appl. Geochem.* **2011**, *26*, 150−151.

(6) Wang, G.-d.; Jiang, M.; Lu, X. g.; Wang, M. Effects of sediment load and water depth on the seed banks of three plant communities in the National Natural Wetland Reserve of Lake Xingkai, China. *Aquat. Bot.* **2013**, *106*, 35−41.

(7) Goldstein, B.; et al. Improve Well Performance by Reducing Formation Damage. In *Unconventional Resources Technology Conference*; Unconventional Resources Technology Conference: San Antonio, Texas, USA, 2015; p 18.

(8) Qutob, H.; Byrne, M. Formation Damage in Tight Gas Reservoirs. In *SPE European Formation Damage Conference and Exhibition*; Society of Petroleum Engineers: Budapest, Hungary, 2015; p 18.

(9) Barker, K. M.; Germer, J. W. Formation Damage in Gas-Storage Wells. In *SPE International Symposium and Exhibition on Formation Damage Control*; Society of Petroleum Engineers: Lafayette: Louisiana, USA, 2010; p 7.

(10) Jia, H.; et al. *Study on Reservoir Protection Workover Fluid System for Dongfang1-1 Gasfield*, 2014; Vol. *29*, pp 93−96.

(11) Lamaka, S. V.; Zheludkevich, M.; Yasakau, K.; Serra, R.; Poznyak, S.; Ferreira, M. Nanoporous titania interlayer as reservoir of corrosion inhibitors for coatings with self-healing ability. *Prog. Org. Coat.* **2007**, *58*, 127−135.

(12) Fleming, N. Technology Focus: Formation Damage. *J. Petrol. Technol.* **2018**, *70*, 69.

(13) Burger, E.; Rebiscoul, D.; Bruguier, F.; Jublot, M.; Lartigue, J.; Gin, S. Impact of iron on nuclear glass alteration in geological repository conditions: A multiscale approach. *Appl. Geochem.* **2013**, *31*, 159−170.

(14) Huang, W.; Peng, P.; Yu, Z.; Fu, J. Effects of organic matter heterogeneity on sorption and desorption of organic contaminants by soils and sediments. *Appl. Geochem.* **2003**, *18*, 955−972.

(15) Hertfelder, G. P.; et al. Are Swelling Elastomer Technology, Pre-perforated Liner and Intelligent Well Technology Suitable Alternatives to Conventional Completion Architecture?. In *SPE/IADC Drilling Conference*; Society of Petroleum Engineers: Amsterdam, The Netherlands, 2007; p 13.

(16) Sadana, A. K.; et al. Water Swell Packers with High Salinity Tolerance and Increased Performance Envelope. In *SPE Middle East Oil & Gas Show and Conference*; Society of Petroleum Engineers: Manama, Kingdom of Bahrain, 2017; p 7.

(17) de Combarieu, G.; Schlegel, M. L.; Neff, D.; Foy, E.; Vantelon, D.; Barboux, P.; Gin, S. Glass−iron−clay interactions in a radioactive waste geological disposal: An integrated laboratory-scale experiment. *Appl. Geochem.* **2011**, *26*, 65−79.

(18) Brooks, R. T. Merging Coiled Tubing and Swellable Packer Technologies. In *Brasil Offshore*; Society of Petroleum Engineers: Macaé, Brazil, 2011; p 7.

(19) Rogers, H. E.; Allison, D.; Webb, E. D. New Equipment Designs Enable Swellable Technology in Cementless Completions. In *IADC/SPE Drilling Conference*; Society of Petroleum Engineers: Orlando, Florida, USA, 2008; p 12.

(20) Jung, H. B.; Kabilan, S.; Carson, J. P.; Kuprat, A. P.; Um, W.; Martin, P.; Dahl, M.; Kafentzis, T.; Varga, T.; Stephens, S.; et al. Wellbore cement fracture evolution at the cement−basalt caprock interface during geologic carbon sequestration. *Appl. Geochem.* **2014**, *47*, 1−16.

(21) Keshka, A. A.-S.; et al. Practical uses of swellpacker technology to reduce water-cut; Case histories. In *Offshore Europe*; Society of Petroleum Engineers: Aberdeen: Scotland, U.K, 2007; p 10.

(22) Dahle, B. O.; et al. First Intelligent Well Completion in the Troll Field Enables Feed-Through Zonal Isolation: A Case History. In *SPE Annual Technical Conference and Exhibition*; Society of Petroleum Engineers: San Antonio, Texas, USA, 2012; p 8.

(23) Kalyani, T.; et al. Swellable Packers in Unique Horizontal Completions Solves Difficult Challenges in Offshore India Vasai East Field. In *Offshore Europe*; Society of Petroleum Engineers: Aberdeen: U.K., 2009; p 12.

(24) Young, D. A.; et al. Openhole ICD Completion With Fracture Isolation in a Horizontal Slimhole Well: Case Study. In *Middle East Drilling Technology Conference & Exhibition*; Society of Petroleum Engineers: Manama, Bahrain, 2009; p 7.

(25) Chen, C.; et al. Application of Smart Packer Technology in Underbalanced Completion. In *IADC/SPE Asia Pacific Drilling Technology Conference and Exhibition*; Society of Petroleum Engineers: Tianjin, China, 2012; p 11.
(26) Song, Z.; Liu, L.; Wei, M.; Bai, B.; Hou, J.; Li, Z.; Hu, Y. Effect of polymer on disproportionate permeability reduction to gas and water for fractured shales. *Fuel* **2015**, *143*, 28−37.
(27) Wurm, R.; Dernovsek, O.; Greil, P. Sol-Gel derived SrTiO3 and SrZrO3 coatings on SiC and C-fibers. *J. Mater. Sci.* **1999**, *34*, 4031−4037.
(28) Chandran, P. L.; Paik, D. C.; Holmes, J. W. Structural mechanism for alteration of collagen gel mechanics by glutaraldehyde crosslinking. *Connect. Tissue Res.* **2012**, *53*, 285−297.
(29) Zhao, M.; Lequeux, F.; Narita, T.; Roché, M.; Limat, L.; Dervaux, J. Growth and relaxation of a ridge on a soft poroelastic substrate. *Soft Matter* **2018**, *14*, 61−72.
(30) Qu, R.; Sun, C.; Ma, F.; Zhang, Y.; Ji, C.; Yin, P. Removal of Fe(III) from ethanol solution by silica-gel supported dendrimer-like polyamidoamine polymers. *Fuel* **2018**, *219*, 205−213.
(31) Brattekås, B.; Pedersen, S. G.; Nistov, H. T.; Haugen, Å.; Graue, A.; Liang, J. T.; Seright, R. S. Washout of Cr(III)-Acetate-HPAM Gels From Fractures: Effect of Gel State During Placement. *SPE Prod. Oper.* **2015**, *30*, 99−109.
(32) Sydansk, R. D. A New Conformance-Improvement-Treatment Chromium(III) Gel Technology. In *SPE Enhanced Oil Recovery Symposium*; Society of Petroleum Engineers: Tulsa, Oklahoma, 1988; p 16.
(33) Wilton, R.; Asghari, K. Improving Gel Performance in Fractures: Chromium Pre-Flush and Overload. *J. Can. Petrol. Technol.* **2007**, *46*, 7.
(34) Kuzmichonok, L.; Asghari, K.; Nakutnyy, P. Performance of Polyacrylamide-Chromium (III) Gel in Carbonate Porous Media: Effect of Source of Crosslinker on Disproportionate Permeability Reduction and Gel Strength. In *Canadian International Petroleum Conference*; Petroleum Society of Canada: Calgary, Alberta, 2007; p 15.
(35) Chester, S. A. Gel Mechanics: A Thermo-mechanically Coupled Theory for Fluid Permeation in Elastomeric Materials. *Procedia IUTAM* **2015**, *12*, 10−19.
(36) Raub, C. B.; Suresh, V.; Krasieva, T.; Lyubovitsky, J.; Mih, J. D.; Putnam, A. J.; Tromberg, B. J.; George, S. C. Noninvasive Assessment of Collagen Gel Microstructure and Mechanics Using Multiphoton Microscopy. *Biophys. J.* **2007**, *92*, 2212−2222.

https://doi.org/10.1021/acsomega.3c02494
ACS Omega 2023, 8, 23112−23119